Chapter 16
What We Learn from *In Vivo* EPR Oxygen Images

Gage Redler, Boris Epel, and Howard J. Halpern

Abstract Distributions of oxygen concentration (pO_2) are a critical determinant of normal tissue health as well as tumor aggressiveness and response to therapy. A number of studies show the value of normal tissue and tumor tissue oxygenation images and some of these will be discussed here. A strong correlation between tumor hypoxic fraction as measured with electron paramagnetic resonance oxygen imaging and radiation treatment success or failure has been found in two separate cancer types. Oxygen images of the torso of wild type mice show initial reduction of lung, liver, visceral, and muscle pO_2 with cyclic halving of fraction of inspired oxygen (FiO_2), but variation is blunted over an hour. Spontaneous breast cancers in Mouse Mammary Tumor Viral (MMTV) promoted-polyoma middle T antigen (PyMT) mice with BNIP3, a major factor in promotion of mitochondrial autophagy, knocked out will be compared with wild type animals. Preliminary studies for the BNIP3 knock out animals show extremely low pO_2. The wide variety of studies, in which oxygen images can play an integral role, serve to demonstrate the importance of oxygen images.

Keywords EPR • Oxygen imaging • Hypoxia • BNIP3 • Cancer • Microenvironment response

G. Redler • B. Epel
Center for EPR Imaging In Vivo Physiology, Chicago, IL, USA

Department of Radiation Oncology, University of Chicago, Chicago, IL, USA

H.J. Halpern (✉)
Center for EPR Imaging In Vivo Physiology, Chicago, IL, USA

Department of Radiation Oncology, University of Chicago, Chicago, IL, USA

MC1105, Department of Radiation and Cellular Oncology, University of Chicago Medical Center, 5841 S. Maryland Ave, Chicago, IL 60637, USA
e-mail: h-halpern@uchicago.edu

H.M. Swartz et al. (eds.), *Oxygen Transport to Tissue XXXVI*, Advances in Experimental Medicine and Biology 812, DOI 10.1007/978-1-4939-0620-8_16,

1 Introduction

In vivo oxygen concentration (pO_2) has been found to be crucially important in determining normal tissue health as well as the aggressiveness of tumors and their response to various forms of treatment [1–4]. Due to the ubiquitous influence of tissue pO_2 various methods for measuring and/or imaging pO_2 have been developed [5–8].

One such method is electron paramagnetic resonance (EPR) oxygen imaging (EPROI). EPROI is a particularly robust method of imaging in vivo tissue pO_2 distributions for several reasons. EPROI provides full 3D images of pO_2. These images have good spatial resolution (~1 mm^3 voxels) as well as pO_2 resolution (1–3 torr). The low electromagnetic wave excitation frequencies (e.g., 250 MHz) currently used in EPRI are comparable to those used in 6T whole body MRI and can penetrate deep in tissue (>7 cm) in animals as large as humans. EPROI images are obtained non-invasively, which means they can be used to study in vivo pO_2 distributions without perturbing the system. EPROI requires an intravenously injected, non-toxic spin probe, which distributes in the extracellular compartment of tumors, to report local pO_2 [9]. The accuracy of EPROI oxygen measurements has been established by correlating with well-established optical fiber based oxygen measurement techniques [10].The information provided by EPROI can be applied to help study myriad interesting oxygen related biologic and physiologic topics. A number of studies demonstrating the array of interesting applications of 3D EPR oxygen images of normal tissue and/or tumor tissue will be presented here.

2 Methods

EPROI is used to non-invasively determine the effect of tumor pO_2 on success of tumor treatment with radiation therapy. Two cancer models are used: fibrosarcoma (FSa) and murine mammary MCa4 carcinoma. Fraction of EPROI voxels with less than 10 torr pO_2 (HF10) is used as a measure of tumor hypoxia. The variable HF10 is then correlated to success or failure of radiotherapy to see what role, if any, hypoxia as determined by EPROI plays in tumor resistance to treatment.

EPROI has been used to provide insight into the effect of fraction of inspired oxygen (FiO_2) changes on the distribution of pO_2 in various organs of mice. The result of cyclic FiO_2 variation can also be observed in various organs using EPROI. This directly assesses levels of tissue pO_2 in models of important disorders such as sleep apnea to understand their biologic effects.

To examine the role of BNIP3 in tumor progression and regulation of oxygenation, changes in pO_2 levels and distributions in mouse mammary tumors are compared for BNIP3 null mice that have been crossed to the Mouse Mammary Tumor Viral (MMTV) promoted-polyoma middle T antigen (PyMT) mouse model of breast cancer and wild type mice. EPROI images are registered with anatomic CT images to analyse differences in oxygenation within these tumors.

3 Results

Using two cancer models (FSa and MCa4), we found that EPROI corroborates the theory that tumors exhibiting a higher degree of hypoxia tend to be more resistant to radiation therapy. A cohort of animals with either of the two tumor lines were treated to the previously determined 50 % tumor control dose (TCD_{50}) for each tumor type. The HF10 as determined by EPROI for each tumor was correlated with radiation therapy treatment outcome. For the FSa tumors, hypoxic tumors (HF10 > 10 %) 37 % were successfully controlled while for tumors with HF10 < 10 %, 90 % were successfully controlled ($p = 0.0138$) [11, 12]. For the MCa4 tumors, hypoxic tumors (HF10 > 10 %) 23 % were successfully controlled while for tumors with HF10 < 10 %, 90 % were successfully controlled ($p = 0.0072$) [12]. An example of the dramatic oxygenation difference observed in animals whose tumors were successfully controlled with radiotherapy versus those for which radiotherapy failed is shown in Fig. 16.1.

Significant differences in the overall pO_2 in three tissue types of a mouse breathing air versus a mouse breathing 12 % O_2 are seen in whole-body EPROI (Fig. 16.2). It is seen that significant variations in tissue pO_2 are observed with oscillating FiO_2, however the response becomes damped over time (Fig. 16.3). The direct assessment of tissue pO_2 responses in vivo provides data concerning the extent of hypoxia induced in these tissues and allows the development of models explaining the deleterious end organ effects.

Preliminary studies of BNIP3 knock out (KO) mice show extremely hypoxic breast tumors (Fig. 16.4). This is consistent with the fact that BNIP3 null tumor cells show increased invasive properties, suggesting that BNIP3 is a metastasis suppressor required to maintain mitochondrial integrity and mitigate against the metastasis promoting activities of reactive oxygen and hypoxia [13].

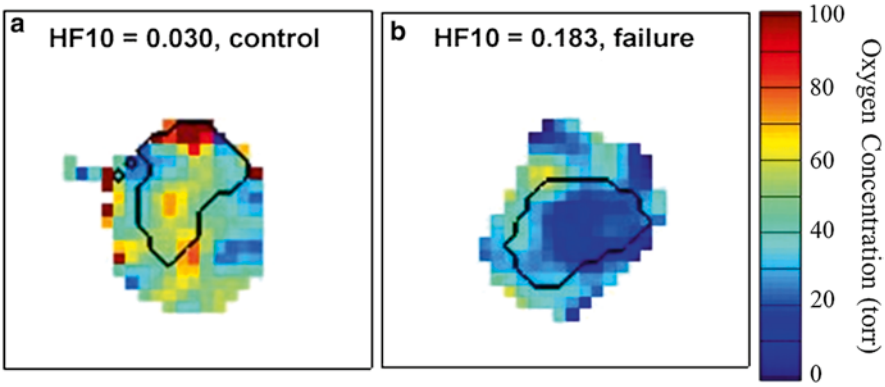

Fig. 16.1 Sample slices from representative EPROI of mouse legs bearing tumors (*black outline*) demonstrating the difference in tumor oxygenation observed in animals where treatment with radiation therapy eventually (**a**) successfully controlled the tumor or (**b**) failed to control the tumor

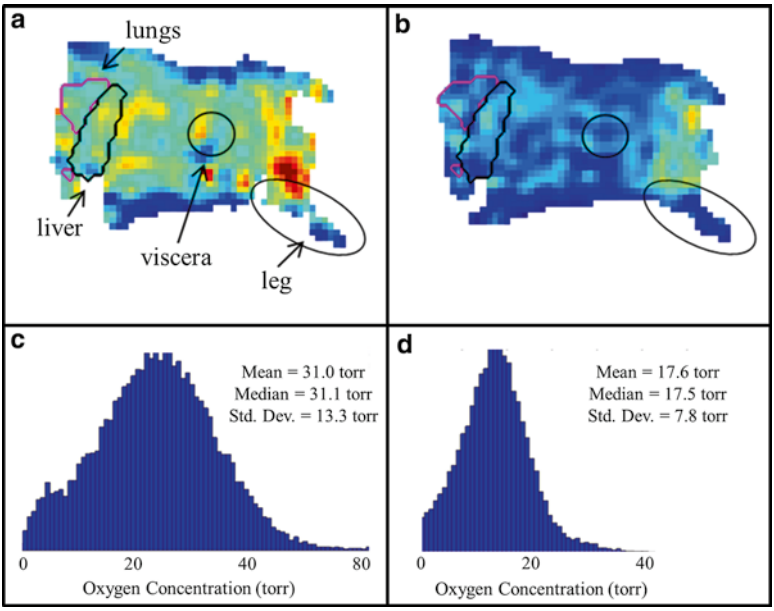

Fig. 16.2 Demonstration of the overall effect on the tissue pO_2 of a mouse when the breathing gas oxygen content is changed from 21 % O_2 to 12 % O_2 as measured with EPROI. Whole body EPROI of a mouse breathing (**a**) 21 % O_2 and (**b**) 12 % O_2, with labeled regions of interest. The pO_2 distributions for the whole body EPROI when the mouse is breathing (**c**) 21 % O_2 and (**d**) 12 % O_2

4 Discussion and Conclusions

With EPROI we can begin to develop quantitative assays of hypoxia induced in tumors and normal tissues. These, in turn will allow the development of quantitative models of the response of tumors and normal tissues to anti-cancer therapies and models of end-organ damage from disease processes such as the intermittent hypoxia induced by sleep apnea.

The hypoxic fraction of a tumor, as determined by EPROI, has been found to be quite a powerful determinant in the eventual outcome of treatment with radiation. This validates EPROI as a tool to analyze spatial distributions of pO_2 in vivo.

In preliminary studies EPROI has also proven to be a valuable tool for tracking tissue pO_2 response to changes in FiO_2. EPROI therefore has the potential to enhance studies investigating the biologic consequences of temporally fluctuating tissue oxygenations (e.g., sleep apnea conditions) by allowing noninvasive tracking of the response to FiO_2 changes of whole body pO_2 as well as pO_2 of individual organs and how this response changes over time.

EPR oxygen images can also help investigate the complicated effects of hypoxia on several aspects of tumor and tissue development. This is evidenced by preliminary results from a study investigating the effect of the BNIP3 protein, which limits

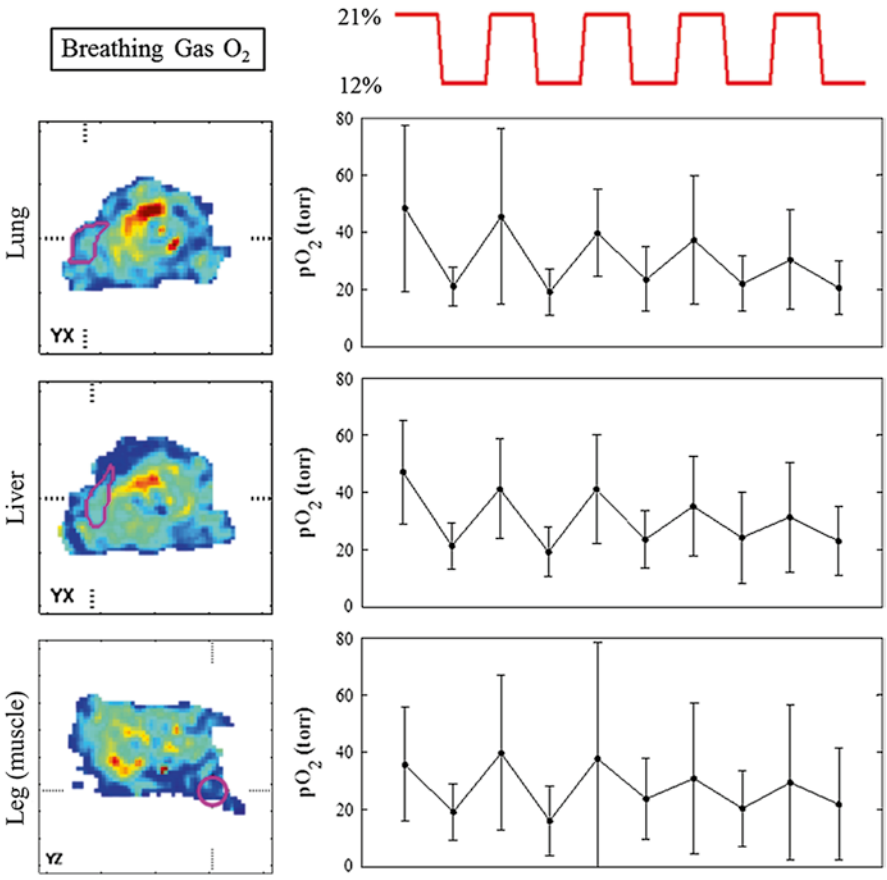

Fig. 16.3 Slices from an EPROI of a mouse are shown with regions of interest outlined in *magenta*. The breathing gas oxygenation for the mouse alternates from 21 % O_2 to 12 % O_2 (breathing gas O_2 changes shown in *red line*). Next to each image with a particular region of interest (lung, liver, or leg muscle) the change in mean oxygenation within that region of interest in response to the breathing gas change is shown

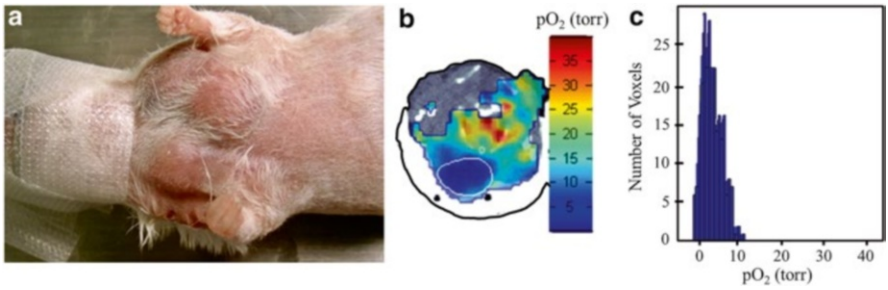

Fig. 16.4 (**a**) Photograph of MMTV-PyMT, BNIP3 null breast cancer tumors grown in the breast of a mouse. (**b**) Registered EPROI overlaid on an anatomical CT of the mouse, shown with the tumor outlined in *white*. (**c**) Distribution of pO_2 found within the BNIP3 null tumor demonstrating that the tumor is extremely hypoxic

production of reactive oxygen species by promoting mitochondrial degradation at the autophagosome, on tumor oxygenation. Initial results show that tumors in BNIP3 KO mice are extremely hypoxic, which may be due to dysfunctional mitochondria. EPROI will help in further studies to investigate the effect of BNIP3 on oxygenation as well as radiation resistance.

In general, oxygen images from EPROI provide an important tool in understanding the relationship between microenvironment oxygenation and a wide variety of crucial physiologic functions.

Acknowledgments Supported by NIH grants P41 EB002034 and R01 CA98575.

References

1. Hockel M, Schlenger K, Aral B et al (1996) Association between tumor hypoxia and malignant progression in advanced cancer of the uterine cervix. Cancer Res 56:4509–4515
2. Shannon AM, Bouchier-Hayes DJ, Condron CM et al (2003) Tumour hypoxia, chemotherapeutic resistance and hypoxia-related therapies. Cancer Treat Rev 29:297–307
3. Carmeliet P, Dor Y, Herbert JM et al (1998) Role of HIF-1alpha in hypoxia-mediated apoptosis. Nature 394:485–490
4. Rofstad EK (2000) Microenvironment-induced cancer metastasis. Int J Radiat Biol 76:589–605
5. Dewhirst MW, Klitzman B, Braun RD et al (2000) Review of methods used to study oxygen transport at the microcirculatory level. Int J Cancer 90:237–255
6. Zhao DW, Jiang L, Mason RP (2004) Measuring changes in tumor oxygenation. Methods Enzymol 386:378–418
7. Tatum JL (2006) Hypoxia: importance in tumor biology, noninvasive measurement by imaging, and value of its measurement in the management of cancer therapy. Int J Rad Biol 82:699–757
8. Bayer C, Vaupel P (2012) Acute versus chronic hypoxia in tumors: controversial data concerning time frames and biological consequences. Strahlenther Onkol 188:616–627
9. Golman K, Petersson JS, Ardenkjaer-Larsen JH et al (2000) Dynamic in vivo oxymetry using overhauser enhanced MR imaging. J Magn Reson Imaging 12:929–938
10. Elas M, Ahn KH, Parasca A et al (2006) Electron paramagnetic resonance oxygen images correlate spatially and quantitatively with oxylite oxygen measurements. Clin Cancer Res 12:4209–4217
11. Elas M, Bell R, Hleihel D et al (2008) Electron paramagnetic resonance oxygen image hypoxic fraction plus radiation dose strongly correlates with tumor cure in FSa fibrosarcomas. Int J Radiat Oncol Biol Phys 71:542–549
12. Elas M, Magwood JM, Butler B et al (2013) EPR oxygen images predict tumor control by a 50 percent tumor control radiation dose. Cancer Res (online and in press)
13. Tracy K, Macleod KF (2007) Regulation of mitochondrial integrity, autophagy and cell survival by BNIP3. Autophagy 3(6):616–619